MATHEMATICAL BIOSCIENCES
AND ENGINEERING
Volume **11**, Number **6**, December **2014**

doi:10.3934/mbe.2014.11.1357

pp. **1357–1373**

A MODEL FOR THE NONLINEAR MECHANISM RESPONSIBLE FOR COCHLEAR AMPLIFICATION

Kimberly Fessel and Mark H. Holmes

Department of Mathematical Sciences
Rensselaer Polytechnic Institute
Troy, NY 12180-3590, USA

(Communicated by Qing Nie)

Abstract. A nonlinear model for the mechanism responsible for the amplification of the sound wave in the ear is derived using the geometric and material properties of the system. The result is a nonlinear beam equation, with the nonlinearity appearing in a coefficient of the equation. Once derived, the beam problem is analyzed for various loading conditions. Based on this analysis it is seen that the mechanism is capable of producing a spatially localized gain, as required by any amplification mechanism, but it is also capable of increasing the spatial contrast in the signal.

1. **Introduction.** The fundamental open question in understanding how we hear concerns the role of a nonlinear feedback mechanism known as the cochlear amplifier. To provide some background on how it works, the cochlea is a fluid-filled tubular structure that is subdivided by a partition. A simplified two-chamber illustration is shown in Fig. 1. The partition is rigid except for a flexible portion that is comprised of the basilar membrane (BM), the organ of Corti, and the tectorial membrane (the latter two are not shown in the figure). Within the organ of Corti there are two types of cells which contain mechanically gated ion channels that are capable of responding to the deformation of the partition. What are called the inner hair cells are responsible for transmitting the sound signal to the brain, while the outer hair cells (OHCs) are responsible for the amplifier. What is of interest here is developing a model for the nonlinear forcing on the BM due to the OHCs and to provide an explanation of how this can give rise to an amplification mechanism.

It is thought that OHC forcing is due to electromotility, which refers to the fact that the length of a OHC changes in response to changes in its receptor potential. The assumption is that these *in vitro* length changes translate into *in vivo* forces on the BM. The origin of this voltage-to-force conversion has been identified as a motor protein known as prestin, which is located in the lateral plasma membrane of the OHCs [4, 14]. Over the past few years, much has been learned about OHC electromotility as well as prestin, and a recent review can be found in [1]. Note that although the consensus is that OHC electromotility is the source of the active hearing system; *how* electromotility affects the BM is still unknown.

Modeling the ear has a long history, going back to (at least) Helmholtz. Several analytic models successfully described the passive cochlear dynamics by the 1980s

2010 *Mathematics Subject Classification.* Primary: 92C10, 74H10; Secondary: 35C20.
Key words and phrases. Cochlear amplification, basilar membrane, nonlinear beam.
The authors are supported by NSF grant DMS-1122279.

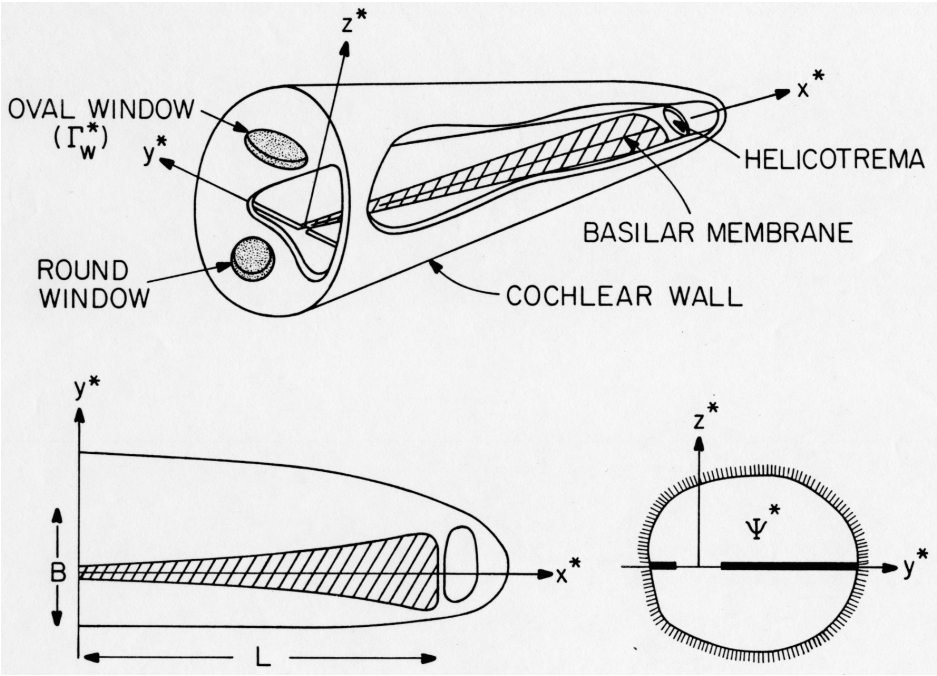

FIGURE 1. The geometry used for modeling of the hearing process is as found in [11]. For the purposes of this paper, the asterisks may be disregarded.

[5, 11, 10, 23]. Since then there has been a considerable effort to derive a model for the amplified cochlea, but with limited success. This is partly due to the incomplete experimental characterization of the mechanism [2], and partly due to the difficulty of analyzing the models that have been proposed. This is not to say that progress has not been made, and significant contributions to the modeling effort include a continuum model by Chadwick [6], the feed-forward model of Steele and his coworkers [16, 26], and the comprehensive models considered by Grosh and his coworkers [20, 17].

In this work we propose a new model for amplification which incorporates the effects of OHC electromotility on the BM. Our assumption is that the force is determined by the displacement of the BM, and the principal nonlinearity comes from the nonlinear dependence of the OHC receptor potential on the deflection of the hair bundle. This differs from the model in [16, 26], where the assumption is made that the amplifier force is proportional to the total vertical force on the partition, while in [6] a wavenumber dependent forcing function is postulated.

To incorporate the nonlinear forcing, we develop a geometric model for the organ of Corti that is based on the work in [7]. With this, the amplification force is decomposed into tangential and normal components, and these are then integrated into a nonlinear beam model for the BM. In the presentation, numerous modeling assumptions are made related to the effective contributions to the amplifier, and reasons are provided for these assumptions. In the end, the essential elements of the model are the nonlinear dynamic tension induced by the OHC forcing, and its strong dependence on the angular deflection of the cilia bundle. It should be pointed

out that it is not assumed that the BM is under tension, but rather that as the BM deflects, the tangential component of the OHC forcing is the principal cause of the amplification mechanism.

What is not considered is how the multi-dimensional fluid loading affects the motion, and this is left for a future study. However, the analysis will provide strong evidence that the proposed mechanism is capable of suppressing the motion of the BM in certain regions, while amplifying it elsewhere. In this sense, it does not simply increase the gain in the region associated with the amplification but it also has the ability to increase the contrast between the amplified and unamplified regions.

2. Cochlear equations of motion.

We consider an uncoiled cochlea which resembles a long, narrow tube. The inside contains two fluid-filled sections separated by a cochlear partition consisting of the basilar membrane and a rigid shelf. Figure 1 depicts this configuration along with the layout for the x-, y-, and z-directions. The length and maximum width of the BM are characterized by the quantities L and B, respectively. The BM width increases with longitudinal position and is thus represented by a x-dependent function. It is also considered to be symmetric about the x-axis. Thus, the BM is located in the $z = 0$ plane and is contained by $0 < x < L$ and $-G(x) < y < G(x)$.

The equations for the cochlear fluid are

$$(\partial_t - \nu\nabla^2)\mathbf{v} = -\frac{1}{\rho}\nabla p, \tag{1}$$

$$\nabla \cdot \mathbf{v} = 0, \tag{2}$$

and for the BM (where $z = 0$)

$$\mathcal{L}(\eta) + \mu\partial_t^2\eta = -[\![p]\!]. \tag{3}$$

In these equations, $\mathbf{v}$ is the velocity, p is the pressure, ν is the kinematic viscosity, ρ is the mass density of the fluid, while η is the z-displacement and μ is the mass per unit area of the BM. Also, $\mathcal{L}$ is a nonlinear beam operator that will be derived shortly, and $[\![p]\!]$ is the pressure jump across the partition.

Given that the principal issue considered here is the nonlinearity associated with amplification, the question arises as to why the convective term in (1) is omitted. The role of compressibility was considered in depth in [15], and the conclusion was that, for the auditory frequency range, it does not significantly affect the motion of the fluid.

2.1. Nonlinear beam model.

The assumption made here is that the OHCs are responsible for in-plane forcing on the BM. The theory used to obtain the resulting equation of motion is based on [8]. To explain, the equations for a beam moving in the y, z-plane are

$$\partial_y^2\zeta + (1+\sigma)\partial_y\eta\partial_y^2\eta = 0, \tag{4}$$

$$EI\partial_y^4\eta - 2hE\big[(1+\sigma)(2\eta_y^2 + \zeta_y)\partial_y^2\eta + \sigma\partial_y\eta\partial_y^2\zeta\big] = (1-\sigma^2)f, \tag{5}$$

where η, ζ are the displacements in the normal (z) and transverse (y) directions, respectively, E is the Young's modulus, $I = 2h^3/3$, $2h$ is the thickness, σ is the Poisson ratio, and f is the normal load. The horizontal traction will be incorporated through the boundary condition. As with the BM, the above equations hold for $-G < y < G$.

Integrating (4), it follows that $\partial_y \zeta + \frac{1}{2}(1+\sigma)(\partial_y \eta)^2 = A$, and integrating this yields

$$\zeta = A_0 y + B_0 - \frac{1}{2}(1+\sigma)\int_{-G}^{G} (\partial_y \eta)^2 dy. \tag{6}$$

Introducing this into (5) we get that

$$EI\partial_y^4 \eta - 2h(1+\sigma)E\left[A_0 + \frac{3}{2}(1-\sigma)(\partial_y \eta)^2\right]\partial_y^2 \eta = (1-\sigma^2)f. \tag{7}$$

It remains to determine A_0, and this is done using the boundary conditions. In terms of its normal displacement, the beam is assumed to be simply supported, so $\eta = \partial_y^2 \eta = 0$ at $y = \pm G$. For the transverse displacement, the beam is assumed fixed at $y = -G$ and there is a loading, due to the OHCs, at $y = G$. Note that the transverse stress is

$$\sigma_y = \frac{E}{1-\sigma^2}(\varepsilon_y + \sigma \varepsilon_z),$$

where $\varepsilon_y = \partial_y \zeta - z\partial_y^2 \eta + \frac{1}{2}(\partial_y \eta)^2$ and $\varepsilon_z = \frac{1}{2}(\partial_y \eta)^2$. Letting P_h denote the imposed stress at $y = G$, then it is found that

$$A_0 = -\frac{1-\sigma^2}{E} P_h.$$

With this, (7) takes the form

$$D\partial_y^4 \eta + \left[P - 3hE(\partial_y \eta)^2\right]\partial_y^2 \eta = f, \tag{8}$$

where $D = EI/(1-\sigma^2)$ is the bending rigidity and $P = 2h(1+\sigma)P_h$. Note that when $P > 0$ the beam is under compression and when $P < 0$ it is under tension. The corresponding solution for the transverse displacement comes form (6), and the boundary condition that requires that $\zeta = 0$ for $y = -G$, and the result is

$$\zeta = -(1-\sigma^2)\frac{P_h}{E}(y+G) - \frac{1}{2}(1+\sigma)\int_{-G}^{G} (\partial_y \eta)^2 dy. \tag{9}$$

The associated strain induced by the lateral load is

$$\varepsilon_h = -(1-\sigma^2)\frac{P_h}{E}. \tag{10}$$

The normal load comes from the fluid as well as the OHCs. Consequently, from (8) we have that (3) can be written as

$$D\partial_y^4 \eta + \left[P - 3hE(\partial_y \eta)^2\right]\partial_y^2 \eta + \mu \partial_t^2 \eta = -[\![p]\!] + K, \tag{11}$$

where K is the normal component of the OHC loading. Assuming the BM is simply supported then the boundary conditions are

$$\eta = \partial_y^2 \eta = 0 \text{ at } y = \pm G(x). \tag{12}$$

The peak amplitude in the unamplified cochlea is determined by the balance between the viscous dissipation and the growth in the wave caused by the gradient in the BM width. Based on preliminary numerical studies for a reduced model, it is expected that the transverse loading plays a more significant role than the normal loading in modifying the properties of the peak amplitude of the wave. Consequently, it is assumed here that $K = 0$, and we concentrate on determining how P depends on η.

3. **Model for micromechanics.** It remains to relate P in (8) to the OHC forcing. This function is determined from the BM displacement and the sequence of events outlining how this happens is shown in Figure 2. The model that is presented does not account for the transients within the respective regimes shown. For example, the deflection of a stereocilia bundle presumably generates viscoelastic and internal forces with the bundle, and these are coupled with related expressions in the other components of the organ of Corti, but these are not accounted for here. The assumption is that displacement of the BM determines the angular deflection uniquely.

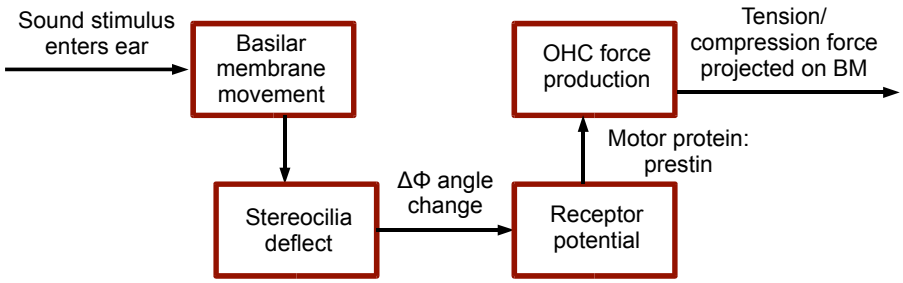

FIGURE 2. A chain of events allows entering sound stimuli to activate OHC electromotility which produces tension/compression force on the basilar membrane.

3.1. **Deflection of stereocilia.** We begin by considering the deflection of the stereocilia as a result of basilar membrane displacement. A schematic of the situation is shown in Figure 3. What is shown is a transverse section within the organ of Corti. We also assume that, at rest, the stereocilia are perpendicular to the reticular lamina (RL). We also group the OHC and its supporting Deiters' cell (DC) into one entity. The DCs have been shown to contain cytoskeletal elements consisting of microtubules and actin fibers which are thought to support the transfer of OHC electromotive forces to the basilar membrane [25], so we assume complete force transmission through the DC is possible.

Figure 3 details the simplified geometric setup of the cross section at rest and during stimulation. The angles ϕ_0, θ_0, ϕ, and θ are defined in the figure. We consider the lengths of the OHC/DC complex (L_1) and the stereocilia (L_2) to be fixed. Although we are modeling the electromotive process which results in OHC length changes *in vitro*, we assume electromotility results in force production *in vivo*. Furthermore, even if OHCs do change their length during stimulation, this length difference is likely small and in-plane with the OHC. We are ultimately interested in the angle ϕ which does not greatly fluctuate in the presence of modest in-plane OHC lengthening/contraction. This being said, we proceed by assuming L_1 is a fixed quantity.

The relative position of three points determine the angular deflection of the stereocilia. These points are the locations where

- the center of the DC base attaches to the BM (P_1),

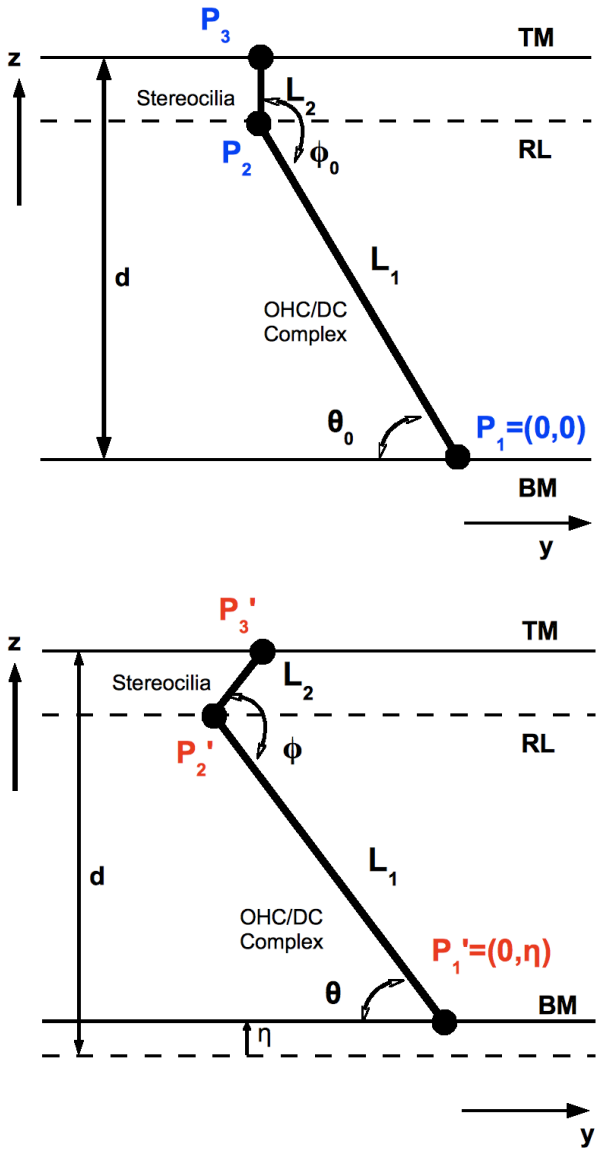

FIGURE 3. This diagram of the cochlear cross section at rest (top) and during stimulation (bottom) provides the basis for our model of the deflection of the stereocilia.

- the bundle connects to the OHC (P_2), and
- the bundle meets the TM (P_3).

In this analysis we set the origin at $P_1 = (0, 0)$. For the stimulated organ of Corti, the points of interest are denoted with apostrophes (P_i' for $i = 1,\ 2,\ 3$). The point $P_1' = (0, \eta)$ is determined by the vertical deflection of the BM at the point of attachment. We assume that the tectorial membrane is stationary. Also, experimental evidence suggests that the OHC stereocilia bundles are wedged into

the TM [9]; therefore, we assume that the point P_3 is fixed ($P_3 = P_3'$). Because the RL is allowed to move, the BM – TM distance change produces a shift of position P_2 and a decrease in the angle ϕ_0. The stereocilia deflection, which determines the flux of ions into the OHC, is characterized by the change in this angle ($\Delta\phi = \phi_0 - \phi$); thus, we now use a geometric argument to determine $\Delta\phi$.

We first solve for ϕ. Consider the triangle formed by joining the vertices P_1', P_2', and P_3'. By the Law of Cosines we find

$$\cos(\phi) = \frac{||P_1' - P_2'||^2 + ||P_2' - P_3'||^2 - ||P_1' - P_3'||^2}{2||P_1' - P_2'||\,||P_2' - P_3'||}.$$

We have fixed lengths for the OHC/DC complex and the stereocilia, so

$$\phi = \arccos\left\{\frac{L_1^2 + L_2^2 - \left[y_3'^2 + (\eta - d)^2\right]}{2L_1L_2}\right\}, \tag{13}$$

where y_3' is the y-coordinate of P_3' and d is the height of the cross section at rest.

Now that we have a complete expression for ϕ, we make a further simplification. The basilar membrane displacement η is much smaller than the other quantities in (13), especially at low-intensity sounds where nonlinearities prove important. For a comparison example consider the guinea pig: the average length of the OHC/DC complex (L_1) is approximately 100 μm; the average stereocilia length (L_2) is 3 μm; but the basilar membrane deflection is only about 1-20 nm for inputs which exhibit significant nonlinearities (less than 60 dB) [19, 22, 24]. To take advantage of this we use a Taylor series approximation for ϕ by expanding around $\eta = 0$. Note that the first term of such an approximation should be ϕ_0, the angle of the complex at rest. It is found that

$$\phi = \phi_0 - \kappa\eta + \mathcal{O}\left(\eta^2\right),$$

where

$$\phi_0 = \frac{\pi}{2} - \arcsin\left[\frac{L_1^2 + L_2^2 - (y_3')^2 - d^2}{2L_1L_2}\right], \tag{14}$$

and

$$\kappa = \frac{2d}{\sqrt{2(L_1^2 + L_2^2)(d^2 + (y_3')^2) - (L_1^2 - L_2^2)^2 - (d^2 + (y_3')^2)^2}}. \tag{15}$$

We are interested in the change in the angle, $\Delta\phi \equiv \phi_0 - \phi$, and from above we have that $\Delta\phi \sim \kappa\eta$. By recalling our assumptions that $P_3' = P_3$ and that the stereocilia are perpendicular to the TM, we can simplify the formula for κ by noting

$$y_3' = y_3 = -L_1\cos(\theta_0), \tag{16}$$

and

$$d = L_2 + L_1\sin(\theta_0). \tag{17}$$

Inserting (16) and (17) into (15), we arrive at the approximation which will be used in the rest of this paper:

$$\Delta\phi \sim \kappa\eta, \tag{18}$$

where

$$\kappa = \frac{L_2 + L_1\sin\theta_0}{L_1L_2\cos\theta_0}.$$

3.2. **Cell receptor potential.** Deflection of the stereocilia bundle modifies the potassium flux into the OHC, and this in turn affects the cell's receptor potential (RP). The nonlinear function relating RP with $\Delta\phi$ has been measured in multiple species, for both inner and outer hair cells [12, 21]. Based on these observations we assume $RP = R_M R(\Delta\phi)$, where R_M is the maximum RP and R has the properties of the function shown in Figure 4. This translates into the requirements that

$$\lim_{\Delta\phi\to\pi/2} R(\Delta\phi) = 1,$$
$$\lim_{\Delta\phi\to-\pi/2} R(\Delta\phi) = -\frac{1}{r},$$

where $r > 1$. We additionally require the value of our function to be zero in the absence of stereocilia deflection, so $R(0) = 0$.

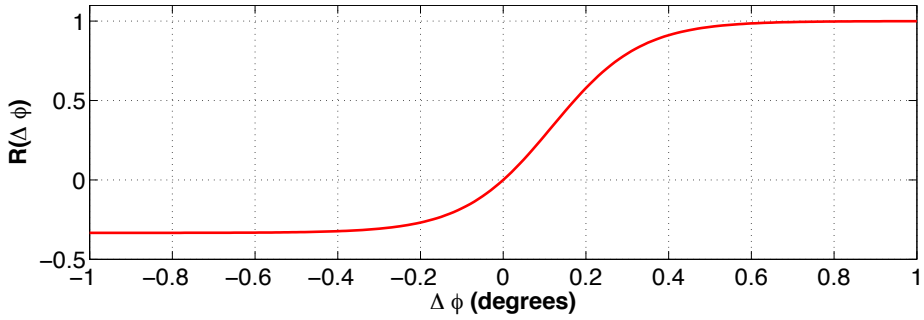

FIGURE 4. Our proposed normalized receptor potential function $R(\Delta\phi)$.

Chadwick uses similar related normalized saturation limits in his model for OHC force production [6], although he assumes $r = 4$. Also, he uses two contrasting hyperbolic tangent functions to achieve these behaviors. We prefer to choose a single continuous function to simplify the analysis. Keeping the requirements in mind, we propose the following function to represent the (normalized) OHC receptor potential:

$$R(\Delta\phi) = R(\kappa\eta) = \frac{1 - e^{-2q\kappa\eta}}{1 + re^{-2q\kappa\eta}}, \tag{19}$$

where q is a constant which controls the steepness of the transition between the two saturations. In most of the calculations that will follow we will take $r = 4$. However, it is of interest to know the relative contributions of the hyperpolarizing and depolarizing phases of the receptor potential, and r will be used to make this determination.

According to the OHC stereocilia bending study of Russell et al. [21], the receptor potential function should saturate with about 25 nm of stereocilia deflection. Given that the average stereocilia considered in that study was 3.5 μm, the change in the angle ϕ which causes saturation ($\Delta\phi_{saturate}$) is characterized as

$$\sin(\Delta\phi_{saturate}) = \frac{25 \text{ nm}}{3500 \text{ nm}}$$

which implies that

$$\Delta\phi_{saturate} \approx 0.409°.$$

By setting $\Delta\phi \sim \kappa\eta = 0.409^\circ$ and assuming saturation of the function ($R_{saturate}$) occurs at 90% receptor potential output, we solve the following equation for q:

$$R_{saturate} = \frac{1 - \exp\{-2q(0.409^\circ)(\pi/180^\circ)\}}{1 + r\exp\{-2q(0.409^\circ)(\pi/180^\circ)\}} = 0.9.$$

Taking $r = 4$, we find that $q = 268$ for R to saturate at 25 nm stereocilia flexion.

3.3. **Outer hair cell force production.** Next we turn our attention toward the amount of force produced by the OHCs. Because of the cochlea's complexity and sensitivity to manipulation, OHC force production as a function of membrane potential change has not been measured *in vivo*. We must, therefore, hypothesize what this functional relationship may be.

Significant effort has been invested in studying the dynamics of OHC motility. In his original OHC electromotility experiments, Ashmore concluded that OHC length changes linearly in response to external command potential for modest inputs [3]. Though he performed his experiment *in vitro* and focused on length–not force–production, Ashmore did report a linear relationship between external stimulus and OHC response. Chadwick assumes a linear relationship between stereocilia bending and OHC force generation in his model for electromotility [6]. In fact, he uses a nonlinear curve similar to $R(\Delta\phi)$ (Figure 4) to form a direct connection between OHC force production and stereocilia bending. More recently, Spector et al. also use a linear relationship to describe the connection between OHC force generation and receptor potential [13].

Here we follow suit by presuming a linear relationship between receptor potential and OHC force production. Let F_{OHC} be the force exerted by one outer hair cell. We know that positive membrane potential contracts the OHC while negative membrane potential causes the OHC to lengthen *in vitro*. *In vivo* this means that the OHC produces force directionally away from the BM for $R > 0$ and toward the BM for $R < 0$. Thus F_{OHC} should have the opposite sign from the receptor potential, and so

$$F_{OHC} = -cR(\Delta\phi), \tag{20}$$

where c is a positive constant with the dimensions of force.

3.4. **Tension on basilar membrane.** Now that the force produced by a OHC has been modeled, we determine how this influence interacts with the basilar membrane. In the previous subsection, we accounted for the directionality of the force; thus, we need only to project it onto the BM.

As explained in Section 2, the tangential component of the OHC force is of interest here. Therefore, let F_{proj} be the projection of the tangential component of the OHC force onto the BM. We find

$$F_{proj} = F_{OHC}\cos\theta, \tag{21}$$

where

$$\cos\theta = \frac{|y_2'|}{L_1}.$$

and y_2' is the y-position of P_2'. Expanding the formula for y_2' for small η, it is found that $\theta \approx \theta_0$ and this approximation will be used in what follows. Also, there are generally three outer hair cells in each mammalian cross section. For simplicity, we assume that the force produced by each OHC is roughly the same and that F_{proj} can be multiplied by a factor of 3 to account for the collective force of the OHCs.

Assuming this force is uniform over the end of the BM then the resulting stress on the BM at $y = G$ is

$$P_h = \frac{3}{4h^2} F_{OHC} \cos\theta_0 \,.$$

3.5. **Summary of nonlinear beam model.** Based on the above modeling assumptions, the resulting equation for the BM is

$$D\partial_y^4\eta + \left[P - 3hE(\partial_y\eta)^2\right]\partial_y^2\eta + \mu\partial_t^2\eta = -[\![p]\!], \tag{22}$$

where

$$P = -P_0 \cos\theta_0 \left[\frac{1 - e^{-2q\kappa\eta_0}}{1 + re^{-2q\kappa\eta_0}}\right], \tag{23}$$

$$\kappa = \frac{L_2 + L_1 \sin\theta_0}{L_1 L_2 \cos\theta_0},$$

$\eta_0 = \eta(x, 0, t)$, and $P_0 = 3c(1 + \sigma)/(2h)$ is a positive constant. Note that the orientation and dimensions of the OHCs vary with longitudinal position in the cochlea, and so κ and θ_0 are functions of x. Also, the BM is located in the $z = 0$ plane, and occupies the region $0 < x < L$, $-G(x) < y < G(x)$. It is assumed simply supported along its lateral edges, and so, the boundary conditions are $\eta = \partial_y^2\eta = 0$ at $y = \pm G$.

There are multiple constants in the function P, and this is significant because it is responsible for the amplification in the model. Most are geometric, such as those used to determine κ, or are known or easily estimated, such as σ. That leaves the two associated with the receptor potential. The value of q was determined using currently available measurements, and it was found that $q = 268$ (assuming $r = 4$). This leaves c, which is associated with the force-receptor potential formula. Although its value is unknown, as will explained below, it is possible to estimate P_0 in (23) using the response of the system to various forcing functions.

In this model for P, we assume a linear relationship between BM displacement and angle deflection and between OHC force production and receptor potential. The crucial nonlinear relationship is between the angular deflection and receptor potential, which gives rise to the exponential functions in (23). Finally, note $P > 0$ results in a lateral compressive force on the BM while $P < 0$ produces a tension force. The presented formulation suggests that the OHCs produce a tension on the BM, and we refer to the OHCs' tangential force as such for the remainder of this work.

4. **Affects of OHC loading.** In the calculations to follow, the material values for a guinea pig are used. Specifically, using the values in [10], $E = 10^9$ dyn/cm^2, $\sigma = 1/2$, $G = B(0.186x + 0.35)$, $h = 8 \times 10^{-4}$ cm, $B = 0.026$ cm, and $L = 1.88$ cm. Also, $L_1 = 100\mu$m, $L_2 = 3\mu$m, $q = 268$, and $\theta_0 = \pi/4$. To explain how the value for F_0 is chosen, for the linear unamplified problem (so $Q = 0$), the centerline displacement of the BM is $5F_0G^4/(24D)$. As observed in [18], in the basal region the displacement of the BM is about 1 nm at 20 dB SPL, about 10 nm at 40 dB SPL, and about 100 nm at 100 dB SPL. To achieve a vertical displacement of 1 nm it is required that $F_0 = 0.7864$ and for 100 nm it is required that $F_0 = 78.64$. The one remaining parameter is $P_0 = 3c(1 + \sigma)/(2h)$, which appears in (23). The constant c comes from the constitutive law for the force produced by the OHCs, and there are no direct experimental observations that can be used to determine c.

However, it is possible to use an indirect approach by considering the strain induced by the OHCs. This is given in (10), and from this it follows that

$$P_0 = \frac{4hE\varepsilon_h}{9(1-\sigma)\cos(\theta_0)}\,. \tag{24}$$

For example, if $\varepsilon_h = 0.01$ then $P_0 = 10^4$.

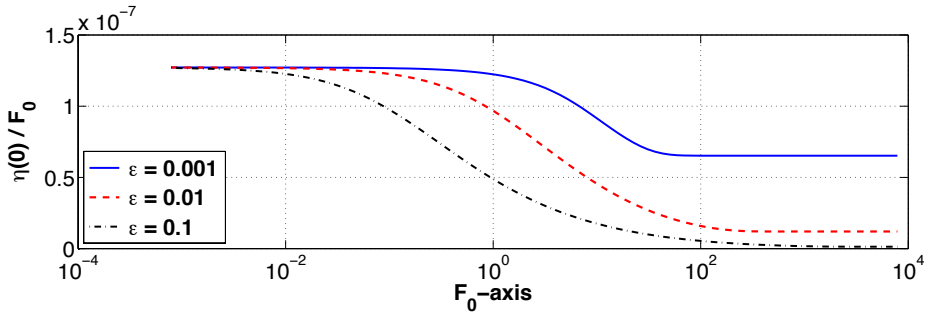

FIGURE 5. Normalized displacement of midpoint of beam as a function of the applied pressure F_0 for different values of the OHC strain ε_h.

4.1. **Uniform pressure.** To examine the consequences of the nonlinear OHC loading we begin with the steady-state response to a uniform pressure. The equation in this case is

$$D\partial_y^4\eta + Q(P,\partial_y\eta)\partial_y^2\eta = F_0, \tag{25}$$

where

$$Q(P,\partial_y\eta) = P - 3hE(\partial_y\eta)^2, \tag{26}$$

P is given in (23), and F_0 is the given constant pressure. The boundary conditions are $\eta = \partial_y^2\eta = 0$ at $y = \pm G$.

The resulting normalized displacement of the midpoint ($y = 0$) of the beam is shown in Figure 5 as a function of the applied pressure F_0. What is also shown are the curves obtained for different values of the induced OHC strain ε_h. What is seen is that the OHC tension acts as a switch. For lower pressures the displacement increases linearly with F_0, and it switches to another linear function at higher pressures. What is also evident is that the tension lowers the displacement. This is expected based on the mechanics but it would seem to be the opposite of what an amplification mechanism should do. What needs to be considered is the dynamic response of the system.

The nonlinearity limits what can be done analytically to examine the dynamic response. To get at an approximate answer, note that because of the small amplitude of the BM that the principal contribution to Q comes from the OHCs. In particular, because of (24), the contributions of the terms in (26) come down to comparing ε_h to $(\partial_y\eta)^2$. Given the small amplitude displacements of the BM it is not unreasonable to assume that $(\partial_y\eta)^2 << \varepsilon_h$, in which case $Q \approx P$. The problem is still nonlinear but it is possible to bound the response by considering the case of when the OHCs are fully engaged, in which case $P = -P_0\cos\theta_0$, and when they are off, which corresponds to $P = 0$. In terms of the wave on the BM, for the passive problem (so $P = 0$) and a pure-tone forcing, the wave grows in amplitude as it moves

down the BM. In reference to Figure 1, the wave moves in the positive x direction. It grows until it almost reaches the location $x = x_r$ where the transverse beam has its fundamental mode equal to the given driving frequency. In fact, without damping in the system, the wave's amplitude becomes unbounded as it approaches x_r. The fluid viscosity prevents this from happening and it dissipates the wave in a small region near x_r. The result is an amplitude that shows a pronounced peak just to the left of x_r. So, one question is, how do the OHCs affect the location of x_r. In the case of constant P, the fundamental mode for the reduced problem has the form $\eta = e^{i\omega t}\cos(\lambda y)$, where $\lambda = \pi/(2G)$ and the associated dispersion relation is $\mu\omega^2 = D\lambda^4 - P\lambda^2$. This can be written as $\omega = M_\infty\omega_0$, where $\omega_0 = \lambda^2\sqrt{D/\mu}$ is the resonant frequency when $P = 0$, and

$$M_\infty = \sqrt{1+\varepsilon}\,, \tag{27}$$

where $\varepsilon = P_0\cos\theta_0/(D\lambda^2)$. Consequently, the tension causes an apical shift in the resonant frequency and the multiplicative factor M decreases as the resonant frequency increases. Also, the value of M_∞ depends on the induced strain ε_h. For example, at $x = L/4 = 0.47$ cm, if $\varepsilon_h = 0.01$ then $M_\infty = 1.7$, while if $\varepsilon_h = 0.001$ then $M_\infty = 1.1$. What this means is that because of the induced tension the wave is able to propagate a bit farther down the BM, and in the process the amplitude is able to grow beyond what it is capable of when $P = 0$. It is also seen that the OHCs do not have to induce much tension in the BM to produce this affect. The verification that this mechanism is capable producing an amplification with the properties observed in the cochlea requires solving the full nonlinear hydroelastic problem, and this will be demonstrated in an upcoming publication.

4.2. **Periodic forcing.** To get a better handle on how the amplifier nonlinearity affects the pure tone response, consider the equation

$$D\partial_y^4\eta + P\partial_y^2\eta + \mu\partial_t^2\eta = F_0\cos(\lambda y)\cos(\omega t), \tag{28}$$

where $\lambda = 2\pi/G$, P is given in (23), and the boundary conditions are $\eta = \partial_y^2\eta = 0$ at $y = \pm G$. The solution can be written as $\eta = \cos(\lambda y)u(t)$, where

$$\mu u'' + \lambda^2(D\lambda^2 - P)u = F_0\cos(\omega t)\,, \tag{29}$$

and

$$P = -P_0\cos\theta_0\frac{1-\exp[-2q\kappa u(t)]}{1+r\exp[-2q\kappa u(t)]}\,.$$

The fundamental frequency for the unamplified problem is $\omega_0 = \lambda^2\sqrt{D/\mu}$. Nondimensionalizing the equation by taking $\tau = \omega_0 t$, and $u = u_c w$ where $u_c = F_0/(D\lambda^4)$, then the above problem can be rewritten as

$$w'' + (1+\varepsilon R)w = \cos[(1+\beta\varepsilon)\tau]\,, \tag{30}$$

where $\varepsilon = P_0\cos\theta_0/(D\lambda^2)$,

$$R = \frac{1-\exp(-\chi w)}{1+r\exp(-\chi w)}\,,$$

and $\chi = 2q\kappa F_0/(D\lambda^4)$. Note that β is a detuning parameter and will be used to determine the resonant frequency for the nonlinear problem.

Multiple-scales can be used to derive an approximate solution of (30), and this is done by introducing the time scales $\tau_1 = \tau$ and $\tau_2 = \varepsilon\tau$, along with the expansion

$w \sim \varepsilon^{-1} w_0(\tau_1, \tau_2) + w_1(\tau_1, \tau_2) + \cdots$. The $O(\varepsilon^{-1})$ equation coming from (30) is $\partial_1^2 w_0'' + w_0 = 0$, where $\partial_1 = \partial_{\tau_1}$. Solving this we have that

$$w_0 = A(\tau_2)\cos[\tau_1 + \phi(\tau_2)]\,. \tag{31}$$

The $O(1)$ equation coming from (30) is

$$\partial_1^2 w_1 + w_1 + 2\partial_1\partial_2 w_0 + R_\infty w_0 = \cos(\tau_1 + \beta\tau_2)\,, \tag{32}$$

where $\partial_2 = \partial_{\tau_2}$. Also, $R_\infty = 1$ if $w_0 > 0$, $R_\infty = -r$ if $w_0 < 0$ and $R_\infty = 0$ if $w_0 = 0$. In preparation for removing the secular producing terms, note that $R_\infty w_0$ is a 2π-periodic function of τ_1. Expanding it in a Fourier series in the form $R_\infty w_0 = \sum[a_n \sin(n\tau_1) + b_n \cos(n\tau_1)]$, then

$$\begin{aligned} a_1 &= \frac{1}{\pi}\int_0^{2\pi} R_\infty w_0 \sin\tau_1 d\tau_1 \\ &= -\frac{1}{\pi r}A\int_{-\phi+\pi/2}^{-\phi+3\pi/2} \cos(\tau_1+\phi)\sin\tau_1 d\tau_1 + \frac{1}{\pi}A\int_{-\phi+3\pi/2}^{-\phi+5\pi/2} \cos(\tau_1+\phi)\sin\tau_1 d\tau_1 \\ &= -\frac{1}{2}(1-r^{-1})A\sin\phi, \end{aligned}$$

and

$$\begin{aligned} b_1 &= \frac{1}{\pi}\int_0^{2\pi} R_\infty w_0 \cos\tau_1 d\tau_1 \\ &= \frac{1}{2}(1-r^{-1})A\cos\phi. \end{aligned}$$

Consequently,

$$\begin{aligned} 2\partial_1\partial_2 w_0 + R_\infty w_0 &= -2A'\sin(\tau_1+\phi) - 2A\phi'\cos(\tau_1+\phi) \\ &\quad - \frac{1}{2}(1-r^{-1})A\sin\phi\sin\tau_1 + \frac{1}{2}(1-r^{-1})A\cos\phi\cos\tau_1 \\ &= 2\left[-A'\cos\phi + A\phi'\sin\phi - \frac{1}{4}(1-r^{-1})A\sin\phi\right]\sin\tau_1 \\ &\quad + 2\left[-A'\sin\phi - A\phi'\cos\phi + \frac{1}{4}(1-r^{-1})A\cos\phi\right]\cos\tau_1. \end{aligned}$$

Removing the secular producing terms yields

$$-A'\cos\phi + A\phi'\sin\phi - \frac{1}{4}(1-r^{-1})A\sin\phi = -\frac{1}{2}\sin(\beta\tau_2),$$

and

$$-A'\sin\phi - A\phi'\cos\phi + \frac{1}{4}(1-r^{-1})A\cos\phi = \frac{1}{2}\cos(\beta\tau_2).$$

These can be rewritten as

$$A' = -\frac{1}{2}\sin(\phi - \beta\tau_2), \tag{33}$$

and

$$A\phi' - \frac{1}{4}(1-r^{-1})A = -\frac{1}{2}\cos(\phi - \beta\tau_2). \tag{34}$$

Assuming the motion begins from rest, then the associated initial conditions are $A(0) = 0$ and $\phi(0) = -\pi/2$. The solution of this nonlinear system is

$$A = \frac{1}{k}\sin\left(\frac{1}{2}k\tau_2\right), \tag{35}$$

$$\phi = \frac{1}{2}\left[\frac{1}{4}\left(1 - \frac{1}{r}\right) + \beta\right]\tau_2 - \frac{\pi}{2}, \tag{36}$$

where $k = \frac{1}{4}\left(1 - r^{-1}\right) - \beta$. To establish the accuracy of this approximation, in Figure 6 the amplitude determined using (35) is compared to the numerical solution of (30). In this case, $\varepsilon = 10^{-2}$, $\lambda = 1$, $\beta = 0$, $r = 4$, and the numerical solution is obtained using the ode45 command in MATLAB.

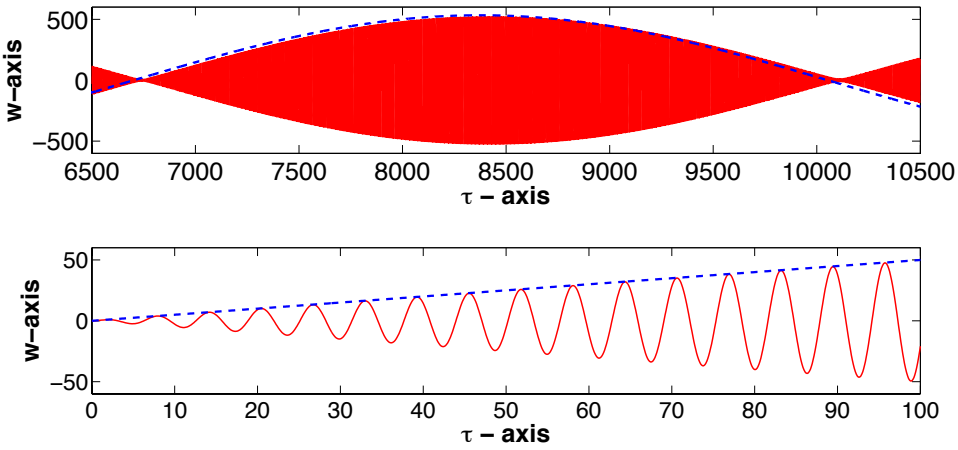

FIGURE 6. Comparison between the numerical solution of (30), solid curve, and the asymptotic approximation for the amplitude given in (35), dashed curve. Two time intervals are shown, the lower graph being the response for smaller values of τ, and the upper graph is for a later time interval.

Returning to dimensional coordinates, the first term approximation of the solution of (29) is

$$u(t) \sim a\sin(b\omega_0 t)\sin[(1+c)\omega_0 t], \tag{37}$$

where

$$a = \frac{F_0}{k\lambda^2 P_0\cos\theta_0} \tag{38}$$

$$b = \frac{kP_0\cos\theta_0}{2D\lambda^2} \tag{39}$$

$$c = \left[\frac{1}{4}\left(1 - \frac{1}{r}\right) + \beta\right]\frac{P_0\cos\theta_0}{2D\lambda^2} \tag{40}$$

and $k = \frac{1}{4}(1 - r^{-1}) - \beta$. From this it is evident that resonance occurs when $k = 0$, which means that $\beta = \frac{1}{4}(1 - r^{-1})$. Consequently, the resonant frequency is $\omega = M\omega_0$

where

$$M = 1 + \frac{1}{4}\left(1 - \frac{1}{r}\right)\varepsilon. \tag{41}$$

Taking $r = 4$, then in comparison to the bound given in (27), this shows that at $x = L/4 = 0.47$ cm, if $\varepsilon_h = 0.01$ then $M_\infty = 1.2$, while if $\varepsilon_h = 0.001$ then $M_\infty = 1.02$. The affect of this magnification factor is shown in Figure 7, which gives the position of the resonant beam as a function of the driving frequency for both an unamplified system as well as two different amplified problems.

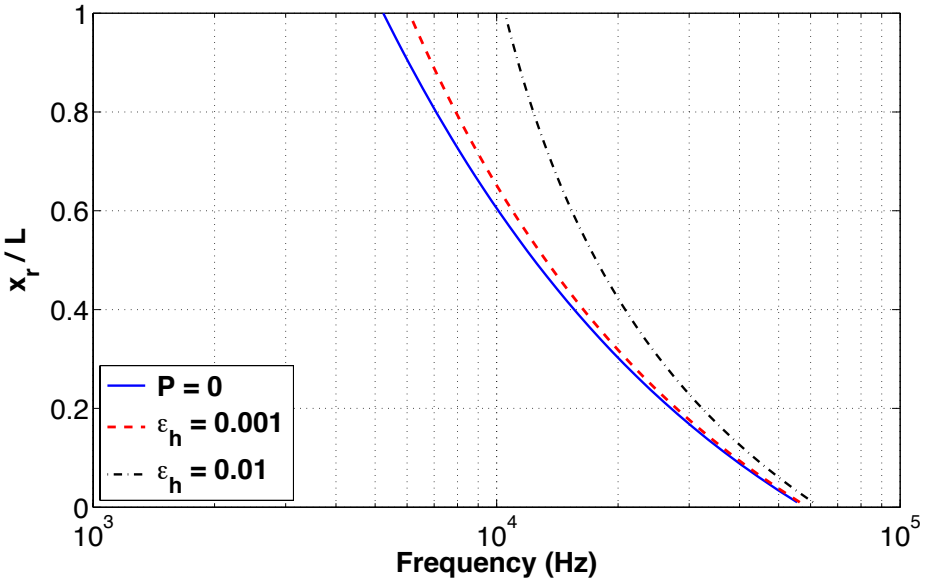

FIGURE 7. Location x_r of resonant beam as a function of the driving frequency, for the unamplified system ($P = 0$) and for the amplified problem for two different OHC strains ε_h.

It is informative to consider how the shift depends on the material parameters. For example, the magnification factor in (41) increases with the imposed OHC strain ε_h. It also depends on the asymmetry of the receptor potential's dependence on the the stereocilia deflection (see Figure 4). Namely, the magnitude of the hyperpolarizing phase is determined by r, which is a measure of the asymmetry in the receptor potential. If the receptor potential is symmetric, so $r = 1$, then from (41) there is no shift in the resonant frequency. Correspondingly, the shift increases as the asymmetry increases. It is also evident that the shift has little dependence on the parameters q and κ, which come from the angular deflection of the stereocilia (23). The reason is that because the system is going into resonance, the amplitude grows to the point that the receptor potential function takes on the characteristics of a switch. Whether this happens when the fluid is included is unclear because the growth in the amplitude is tempered by the dissipation, and so it will depend on the balance between the dissipation and resonant effect.

5. **Discussion.** A model for the amplification mechanism has been proposed. The underlying assumption is that the OHCs are responsible for producing a force on

the BM and we decomposed this into normal and tangential components. The nonlinearity in the force comes from the dependence of the receptor potential on the angular deflection of the OHCs stereocilia. In particular, because of the small amplitudes involved, it is assumed that the force produced by the OHCs depends linearly on the receptor potential, and the angular deflection depends linearly on the displacement of the BM. The result is a nonlinear beam equation for the deflection of the BM.

It was found that the tension induced by the OHCs has the ability to reduce the displacement of the BM. For example, this is evident in (38), which shows that the amplitude decreases with P_0. However, the amplitude becomes unbounded as the resonant frequency is approached. The induced tension in this case shifts the resonant frequency, the shift depending on the tension. It is this shift that is proposed to produce the increase gain due to the amplifier. The reason is that the wave's amplitude grows as it propagates down the BM, and this is due to the increase in the width of the BM. By enabling the wave to go a bit further, the wave continues to grow before being rapidly dissipated by the fluid viscosity. Consequently, the proposed mechanism has the capability to reduce the BM displacement in one region yet increase it in another. In other words, it has the ability to modify both the gain and contrast of the response. Whether this is consistent with experimental observation requires solving the problem with the fluid included, and this will appear in a future study.

Acknowlegments. This work was supported, in part, by the NSF through grant DMS-1122279.

REFERENCES

[1] J. Ashmore, Cochlear outer hair cell motility, *Physiol. Rev.*, **88** (2008), 173–210.
[2] J. Ashmore, P. Avan, W. E. Brownell, P. Dallos, K. Dierkes, R. Fettiplace, K. Grosh, C. M. Hackney, A. J. Hudspeth, F. Jülicher, B. Lindner, P. Martin, J. Meaud, C. Petit, J. R. Santos Sacchi and B. Canlon, The remarkable cochlear amplifier, *Hearing Res.*, **266** (2010), 1–17.
[3] J. F. Ashmore, A fast motile response in guinea-pig outer hair cells: The cellular basis of the cochlear amplifier, *J. Physiol.*, **388** (1987), 323–347.
[4] I. A. Belyantseva, H. J. Adler, R. Curi, G. I. Frolenkov and B. Kachar, Expression and localization of prestin and the sugar transporter glut-5 during development of electromotility in cochlear outer hair cells, *J. Neurosci.*, **20** (2000), RC116.
[5] R. S. Chadwick, Studies in cochlear mechanics, in *Mathematical Modeling of the Hearing Process* (eds. M. H. Holmes and L. A. Rubenfeld), Lecture Notes in Biomathematics, Springer-Verlag, New York, 1981, 369–386.
[6] R. S. Chadwick, Compression, gain, and nonlinear distortion in an active cochlear model with subpartitions, *Proc. Nat. Acad. Sci.*, **95** (1998), 14594–14599.
[7] P. Dallos and B. Fakler, Prestin, a new type of motor protein, *Nature Reviews Molecular Cell Biology*, **3** (2002), 104–111.
[8] D. Y. Gao, Nonlinear elastic beam theory with application in contact problems and variational approaches, *Mech. Res. Commun.*, **23** (1996), 11–17.
[9] R. Glueckert, K. Pfaller, A. Kinnefors, A. Schrott-Fischer and H. Rask-Andersen, High resolution scanning electron microscopy of the human organ of Corti: A study using freshly fixed surgical specimens, *Hearing Res.*, **199** (2005), 40–56.
[10] M. H. Holmes, Frequency discrimination in the mammalian cochlea: Theory vs. experiment, *J. Acoust. Soc. Amer.*, **81** (1987), 103–114.
[11] M. H. Holmes and J. D. Cole, Cochlear mechanics: Analysis for a pure tone, *J. Acoust. Soc. Amer.*, **76** (1984), 767–778.
[12] A. J. Hudspeth and D. P. Corey, Sensitivity, polarity, and conductance change in the response of vertebrate hair cells to controlled mechanical stimuli, *Proc. Nat. Acad. Sci.*, **74** (1977), 2407–2411.

[13] Z. Liao, S. Feng, A. S. Popel, W. E. Brownell and A. A. Spector, Outer hair cell active force generation in the cochlear environment, *J. Acoust. Soc. Amer.*, **122** (2007), 2215–2225.
[14] M. C. Liberman, J. Gao, D. Z. He, X. Wu, S. Jia and J. Zuo, Prestin is required for electromotility of the outer hair cell and for the cochlear amplifier, *Nature*, **419** (2002), 300–304.
[15] J. Lighthill, Energy flow in the cochlea, *J. Fluid Mechanics*, **106** (1981), 149–213.
[16] K. M. Lim and C. R. Steele, A three-dimensional nonlinear active cochlear model analyzed by the WKB-numeric method, *Hearing Res.*, **170** (2002), 190–205.
[17] J. Meaud and K. Grosh, Response to a pure tone in a nonlinear mechanical-electrical-acoustical model of the cochlea, *Biophysical Journal*, **102** (1996), 1237–1246.
[18] K. E. Nilsen and I. J. Russell, The spatial and temporal representation of a tone on the guinea pig basilar membrane, *Proc. Natl. Acad. Sci.*, **97** (2006), 11751–11758.
[19] J. O. Pickles, *An Introduction to the Physiology of Hearing*, Emerald Group, Bingley, UK, 2008.
[20] S. Ramamoorthy, N. V. Deo and K. Grosh, A mechano-electro-acoustical model for the cochlea: Response to acoustic stimuli, *JASA*, **121** (2007), 2758–2773.
[21] I. J. Russell, A. R. Cody and G. P. Richarson, The responses of inner and outer hair cells in the basal turn of the guinea-pig cochlea and in the mouse cochlea grown in vitro, *Hearing Res.*, **22** (1986), 199–216.
[22] I. J. Russell and K. E. Nilsen, The location of the cochlear amplifier: Spatial representation of a single tone on the guinea pig basilar membrane, *Proc. Nat. Acad. Sci.*, **94** (1997), 2660–2664.
[23] C. R. Steele and L. A. Taber, Comparison of WKB calculations and experimental results for three-dimensional cochlear models, *J. Acoust. Soc. Amer.*, **65** (1979), 1007–1018.
[24] I. U. Teudt and C.-P. Richter, The hemicochlea preparation of the guinea pig and other mammalian cochleae, *J. Neurosci. Methods*, **162** (2007), 187–197.
[25] J. A. Tolomeo and M. C. Holley, Mechanics of microtubule bundles in pillar cells from the inner ear, *Biophys. J.*, **73** (1997), 2241–2247.
[26] Y. Yoon, S. Puria and C. R. Steele, Frequency and spatial response of basilar membrane vibration in a three-dimensional gerbil cochlear model, *J. Mech. Mater. Struct.*, **2** (2007), 1449–1458.

Received September 06, 2013; Accepted July 28, 2014.

E-mail address: fessek@rpi.edu
E-mail address: holmes@rpi.edu